Diffusiophoretic and diffusioosmotic velocities for mixtures of valence-asymmetric electrolytes

Ankur Gupta, Bhargav Rallabandi, and Howard A. Stone

Phys. Rev. Fluids **4**, 043702 — Published 12 April 2019

DOI: 10.1103/PhysRevFluids.4.043702

Diffusiophoretic and Diffusioosmotic Velocities for Mixtures of Valence-Asymmetric Electrolytes

Ankur Gupta,[1] Bhargav Rallabandi,[2,1] and Howard A. Stone[1,*]

[1] *Department of Mechanical and Aerospace Engineering, Princeton University, Princeton NJ 08544*
[2] *Department of Mechanical Engineering, University of California Riverside, Riverside CA 92521*

(Dated: March 15, 2019)

Diffusiophoresis and diffusioomosis are electrokinetic phenomena where relative motion is induced between a charged surface and a surrounding electrolyte due to a concentration gradient of ions. In the literature, a relative velocity between a surface and the electrolyte has been derived for a valence-symmetric ($z:z$) electrolyte. In this article, we reformulate the governing equations in a convenient form based on a systematic generalization of the nonlinear Poisson–Boltzmann equations in the limit of a thin double layer, which allows us to derive results for diffusiophoretic and diffusioosmotic velocities for a mixture of electrolytes with a general combination of cation and anion valences. We find that the relative motion depends significantly on ion valences. We also provide analytical approximations for the diffusiophoretic and diffusioosmotic velocities, and discuss their accuracy and applicability. Further, we tabulate diffusiphoretic velocities for some common cases, which highlights the importance of asymmetry in cation and anion valences. Finally, we discuss the validity of our assumptions and the importance of effects such as finite ion size, dielectric decrement and surface conduction for typical experimental conditions.

I. INTRODUCTION

Several physical scenarios involve an electrolyte in the vicinity of a charged surface, such as (i) charging and discharging of double layers, which is the underlying process in electrochemical capacitors [1, 2], (ii) electrophoresis and electroosmosis, which are electrokinetic phenomena where relative motion is induced between the surface and the electrolyte due to the application of an external electric field [3–5], and (iii) diffusiophoresis and diffusioosmosis, which are electrokinetic phenomena where relative motion is induced between the surface and the electrolyte due to a concentration gradient of ions [5, 6]. In this article, we focus on diffusiophoresis and diffusioosmosis, which are observed in processes such as dialysis [7], sedimentation and centrifugation [8], and the motion of colloidal particles in microchannels [9–16]. Moreover, reports in the literature have utilized diffusiophoresis and diffusioosmosis for applications in water treatment [10], fabric cleaning [17], self-propelling 'active' swimmers [18–20], and measurement of the surface zeta potential [21], among others.

Diffusiophoresis is defined as the movement of a charged particle while the surrounding electrolyte is stationary. In contrast, diffusioosmosis occurs when the electrolyte is moving while the surface is stationary. In their classical work, Prieve, Anderson and others derived an expression for the relative velocity for a valence-symmetric electrolyte, or a $z:z$ electrolyte, such as NaCl ($z=1$) and $CaSO_4$ ($z=2$) [5, 6, 22]. They showed that the diffusiophoretic (or diffusioosmotic) velocity is the sum of an electrophoretic component and a chemiphoretic component. In their derivation, a restriction is not imposed on the potential drop across the double layer, or zeta potential ψ_D. However, their analyses require knowledge of the potential variation inside the double layer, first derived by Gouy for a $z:z$ electrolyte [23], to arrive at the expression for the diffusiophoretic velocity. Though there has been an increase in interest to derive results for a mixture of electrolytes with a general combination of cation and anion valences [24–26] a complete solution of the potential inside the double layer is not readily available for a mixture of valence-asymmetric electrolytes. Some authors report an expression for a particle's diffusiophoretic velocity in a mixture of electrolytes where the potential distribution can be evaluated [24, 27] , although their results are only valid in the Debye–Hückel limit of $\Psi_D = \frac{e|\psi_D|}{k_B T} \ll 1$, where Ψ_D is the dimensionless zeta potential, e is the charge on an electron, k_B is the Boltzmann constant, and T is the temperature. However, typical experiments include $\psi_D \lesssim 100$ mV, or $\Psi_D \lesssim 4$ [21]. Therefore, it is necessary to go beyond the limit of $\Psi_D \ll 1$.

Recently, we demonstrated that unequal cation and anion valences influence diffuse-charge relations for an electrolyte near a charged surface [26]. Here, we extend the analysis to calculate the diffusiophoretic and diffusioosmotic

* hastone@princeton.edu

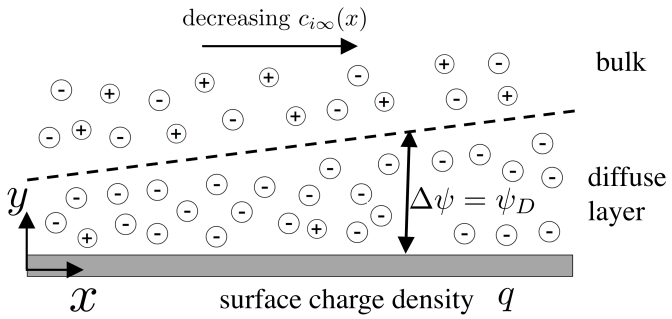

FIG. 1. Sketch and notation for the derivation of the diffusioosmotic velocity. The valence of the i^{th} ion is denoted as z_i, where $z_i > 0$ for a cation and $z_i < 0$ for an anion, here illustrated in shorthand by $\oplus$ and $\ominus$ respectively. The concentration gradient of ions in the x direction induces a relative motion between the electrolyte and the surface. The surface charge density is assumed to be constant and is denoted as q (the schematic shows the scenario of $q > 0$).

velocities. First, we reformulate the classical derivation of the diffusiophoretic velocity and show, perhaps suprisingly, that the detailed profile of the electric potential within the double layer is not necessary to determine the diffusiophoretic velocity. We derive velocities for a general mixture of ions with valence z_i, without imposing any restriction on ψ_D, in the limit of thin double layers. We show that the relative velocity can be significantly influenced by the valence z_i. Our results are in agreement with those previously reported in the Debye–Hückel limit [24, 27], and we also report simplified expressions valid for large zeta potentials. For the case of a single electrolyte with the same valence, we recover the original solution highlighting the generality of our approach.

We derive our main results in the limit of thin double layers and do not consider effects such as finite ion size [26, 28, 29], dielectric decrement [26, 30, 31] and surface conduction [32–34]. Therefore, we discuss experimental conditions where our analysis is applicable and also detail scenarios where the inclusion of the aforementioned effects should be considered.

II. PHYSICAL ORIGIN OF DIFFUSIOPHORESIS AND DIFFUSIOOSMOSIS

We first summarize the physical mechanism that gives rise to diffusiophoresis and diffusioosmosis. For convenience, we only describe the mechanism of diffusioosmosis. A schematic of diffusioosmosis is provided in Fig. 1 where a mixture of electrolytes is in contact with a charged surface. The valence of an i^{th} ion is denoted as z_i. Diffusioosmotic motion of the electrolyte is produced when a gradient in ion concentrations is present far away from the surface, or $c_{i\infty}(x)$ (a more rigorous definition of $c_{i\infty}(x)$ is provided in the next section). Depending on the charge of the surface, either cations or anions are attracted towards the surface, and the concentration of the attracted ion increases significantly near the wall. The length scale of this diffuse-charge region is given by the Debye length, λ_D. Most studies assume a single electrolyte with equal valences of cations and anions, while we focus on the general case of a mixture of multiple electrolytes with arbitrary z_i.

The diffusioosmotic velocity is commonly described as the sum of an electrophoretic component and a chemiphoretic component. We first focus on the electrophoretic component. Due to a gradient in the electrolyte concentration far away from the surface, ions diffuse towards the region of low concentration. However, different mobilities of cations and anions give rise to an electric field to maintain a zero flux of net charge. Since the double layer has a net charge, this electric field creates an electrostatic force inside the double layer. Therefore, the fluid far away from the surface moves so as to generate the shear forces in the double layer that balance the electrostatic forces, similar to an electrophoretic system. In contrast, chemiphoretic movement of the fluid far away from the surface generates shear forces inside the double layer that balance the pressure forces inside the double layer, which arise due to variation in electrical force along the x direction. Depending on the charge at the surface and the relative diffusivities of cations and anions, the electrophoretic and chemiphoretic components can either be in the same direction or in the opposite direction.

III. ANALYSIS OF A GENERAL MIXTURE OF ELECTROLYTES

A. Governing Equations

We assume that the liquid far away from the stationary surface in Fig. 1 contains multiple ions where $z_i > 0$ for a cation and $z_i < 0$ for an anion. Here, x denotes the coordinate along the surface and y is normal to the surface. The surface charge density q is assumed to be constant and is related to the potential drop across the double layer, denoted here as ψ_D (Fig. 1). The incompressible fluid flow is governed by the Stokes equations with an electrostatic body force, Gauss's law of electrostatics, and the Nernst–Planck equations for the flux of ions. We define $\mathbf{u} = u_x(x,y)\mathbf{e}_x + u_y(x,y)\mathbf{e}_y$ as the velocity field, $p(x,y)$ as pressure, μ as the fluid viscosity, $\rho_e(x,y) = e\sum_i z_i c_i$ as the charge density, $\psi(x,y)$ as the electrical potential, $c_i(x,y)$ as the concentrations of the i^{th} ion, $\mathbf{j}_i = j_{ix}(x,y)\mathbf{e}_x + j_{iy}(x,y)\mathbf{e}_y$ as the fluxes of the i^{th} ion, and D_i as the diffusivity of the i^{th} ion. Then, the governing equations are

$$\nabla \cdot \mathbf{u} = 0, \tag{1a}$$

$$-\nabla p + \mu \nabla^2 \mathbf{u} - \rho_e \nabla \psi = \mathbf{0}, \tag{1b}$$

$$-\nabla \cdot (\varepsilon \nabla \psi) = \rho_e = e\sum_i z_i c_i, \tag{1c}$$

$$\nabla \cdot \mathbf{j}_i = 0, \tag{1d}$$

$$\mathbf{j}_i = -D_i \nabla c_i + \mathbf{u} c_i - \frac{D_i z_i e c_i}{k_B T} \nabla \psi. \tag{1e}$$

In the description used above, the electrical permittivity ε is assumed constant.

Our objective is to solve for the diffusioosmotic velocity u_{DO} parallel to the surface, that develops at the outer boundary of the double layer. We first non-dimensionalize the equations. We define a diffusivity scale D^* and an ion concentration scale c^*, which are typical values of ion diffusivities and ion concentration in bulk. There are two relevant length scales in our system. First, there is the length at which the ion concentration changes in bulk, which we denote here as a^*. The second relevant length scale is the Debye length $\lambda_D = \sqrt{\frac{\varepsilon k_B T}{e^2 c^*}}$. We define the thermal potential as $\psi_T = \frac{k_B T}{e}$, $\delta = \frac{\lambda_D}{a^*}$, and a dimensionless surface charge $Q = \dfrac{q}{ec^*\lambda_D}$.

We non-dimensionalize the equations by introducing the dimensionless quantities $X = \frac{x}{a^*}$, $Y = \frac{y}{\lambda_D}$, $C_i = \dfrac{c_i}{c^*}$, $\mathcal{D}_i = \dfrac{D_i}{D^*}$, $\mathbf{U} = \frac{a^*\mu}{\varepsilon\psi_T^2}\mathbf{u}$, $\mathbf{J}_i = \frac{a^*}{\mathcal{D}^* c^*}\mathbf{j}_i$, $P = \frac{\lambda_D^2}{\varepsilon\psi_T^2}p$, $\Psi = \frac{\psi}{\psi_T}$ and $\alpha = \frac{\varepsilon\psi_T^2}{\mu\mathcal{D}^*}$. We note that α is a characteristic Péclet number for the flow outside the double layer and the typical value of $\alpha = \mathcal{O}\left(10^{-1}\right)$. Thus, Eqs. (1) reduce to

$$\hat{\nabla} \cdot \mathbf{U} = 0, \tag{2a}$$

$$-\hat{\nabla} P + \delta \hat{\nabla}^2 \mathbf{U} + \hat{\nabla}^2 \Psi \hat{\nabla} \Psi = \mathbf{0}, \tag{2b}$$

$$-\hat{\nabla}^2 \Psi = \sum_i z_i C_i, \tag{2c}$$

$$\hat{\nabla} \cdot \mathbf{J}_i = 0, \tag{2d}$$

$$\mathbf{J}_i = -\delta^{-1}\mathcal{D}_i \hat{\nabla} C_i + \alpha \mathbf{U} C_i - \delta^{-1}\mathcal{D}_i z_i C_i \hat{\nabla}\Psi, \tag{2e}$$

where $\hat{\nabla} = \lambda_D \nabla = \mathbf{e}_x \delta \frac{\partial}{\partial X} + \mathbf{e}_y \frac{\partial}{\partial Y}$ is the rescaled gradient operator.

B. The Thin Double Layer Approximation

We analyze the system of Eqs. (2) in the limit of $\delta \to 0$, for which the solution is thus divided into two regions: the double layer region and the bulk region [5, 6, 35]. For a formal treatment of these regions through asymptotic analysis, we refer the readers to Schnitzer and Yariv [33].

1. Analysis in the Double Layer

Inside the double layer, since $x = \mathcal{O}(a^*)$ and $y = \mathcal{O}(\lambda_D)$, the dimensionless $X = \mathcal{O}(1)$ and $Y = \mathcal{O}(1)$. We now use order-of-magnitude analysis to simplify Eqs. (2). Using Eq. (2a), we conclude $\frac{U_Y}{U_X} = \mathcal{O}(\delta)$. Similarly, Eq. (2d) suggests that $\frac{J_{iY}}{J_{iX}} = \mathcal{O}(\delta)$. In the limit of $\delta \to 0$, these relations suggest that velocity and species flux in the Y direction are negligible when compared to their values in X direction. However, Eq. (2e) suggests an opposite relation between J_{iY} and J_{iX}. Assuming $C_i = \mathcal{O}(1)$, $\Psi = \mathcal{O}(1)$ and $\alpha \lesssim \mathcal{O}(1)$, we can estimate $\frac{J_{iY}}{J_{iX}} = \mathcal{O}(\delta^{-1})$. Therefore, for the order of magnitude predictions between Eq. (2e) and Eq. (2d) to be consistent with each other and the condition of zero normal flux at $Y = 0$, the dominant terms in J_{iY} from Eq. (2e) must vanish. Thus, the diffusion and electromigration normal to the surface are in balance ($\delta^{-1}\mathcal{D}_i \frac{\partial C_i}{\partial Y} + \delta^{-1} z_i \mathcal{D}_i C_i \frac{\partial \Psi}{\partial Y} = 0$), which upon integration yields

$$C_i = C_{i\infty} \exp(-z_i(\Psi - \Psi_\infty)), \tag{3}$$

where we have defined $C_{i\infty}(X)$ and $\Psi_\infty(X)$ as the concentration of an i^{th} ion and the electrical potential, respectively, far away from the surface, or in the bulk. For convenience, we define $\Psi(X, Y) = \Psi_0(X, Y) + \Psi_\infty(X)$, to get

$$C_i = C_{i\infty} \exp(-z_i \Psi_0). \tag{4}$$

Eq. (4) is the well-known Boltzmann distribution. We note that $\Psi_0(X, 0) = \Psi_D$ is, by definition, the surface (zeta) potential relative to the bulk.

Next, we focus on Eq. (2c): since X and Y are both $\mathcal{O}(1)$ in the Debye layer, $\hat{\nabla}^2 = \delta^2 \frac{\partial^2}{\partial X^2} + \frac{\partial^2}{\partial Y^2} \approx \frac{\partial^2}{\partial Y^2}$, leading to

$$\frac{\partial^2 \Psi}{\partial Y^2} = \frac{\partial^2 \Psi_0}{\partial Y^2} = -\sum_i z_i C_i. \tag{5}$$

Substituting Eq. (4) in Eq. (5) and integrating once while utilizing the matching condition $\frac{\partial \Psi_0}{\partial Y}\big|_{Y\to\infty} = 0$ [33], we get

$$\left(\frac{\partial \Psi_0}{\partial Y}\right)^2 = 2 \sum_i C_{i\infty} g_i(\Psi_0), \tag{6}$$

where we define

$$g_i(\Psi_0) \equiv \exp(-z_i \Psi_0) - 1. \tag{7}$$

We note that $g_i(\Psi_0)$ is the excess concentration of the i^{th} ion in the double layer relative to the bulk.

The typical solution strategy at this stage is to integrate Eq. (6) to find the potential $\Psi_0(X, Y)$. However, analytical solutions are only possible for $z : z$ electrolytes or in the limit of small potentials. Below we develop an alternative method that circumvents this step to address the general case of electrolyte mixtures. Gauss's law at the surface, i.e. $y = 0$, defines the surface charge $q = -\varepsilon \left.\frac{\partial \psi}{\partial y}\right|_{y=0}$, which in dimensionless variables is $Q = -\left.\frac{\partial \Psi}{\partial Y}\right|_{Y=0}$. We utilize Eq. (6) to relate Q to Ψ_D as

$$Q = -\left.\frac{\partial \Psi}{\partial Y}\right|_{Y=0} = \text{sgn}(\Psi_D) \left(2 \sum_i C_{i\infty} g_i(\Psi_D)\right)^{1/2}. \tag{8}$$

Since we have solved for C_i (Eq. (4)) and $\frac{\partial \Psi}{\partial Y}$ (Eq. (6)), we now focus on Eq. (2b) and utilize an order-of-magnitude analysis. In the Y direction, the ratio of shear stress to the electrostatic term is $\mathcal{O}(\delta U_Y) \ll 1$ and therefore, to satisfy Eq. (2b), the pressure term balances the electrostatic term, or

$$\frac{\partial P}{\partial Y} = \frac{\partial^2 \Psi_0}{\partial Y^2} \frac{\partial \Psi_0}{\partial Y}. \tag{9}$$

One integration in Y, along with $P(X, Y \to \infty) = 0$ (choosing the bulk pressure as a reference) and the matching condition $\frac{\partial \Psi_0}{\partial Y}\big|_{Y\to\infty} = 0$, yields

$$P(X, Y) = \frac{1}{2}\left(\frac{\partial \Psi_0}{\partial Y}\right)^2 = \sum_i C_{i\infty} g_i(\Psi_0). \tag{10}$$

Physically, Eq. (10) states the well-known idea that the osmotic pressure inside the double layer is higher than that in the bulk due to the electric field inside the double layer. Therefore, $\sum_i C_{i\infty} g_i(\Psi_0)$ is a measure of the rescaled energy density inside the double layer.

Given the form of Eq. (10) in terms of Ψ_0, it is useful to change independent variables to express $P(X,Y) = \tilde{P}(C_{i\infty}(X), \Psi_0(X,Y))$; note that there is no loss of generality in this transformation within the thin Debye layer approximation used here. Thus, we may write

$$\left.\frac{\partial P}{\partial X}\right|_Y = \sum_i \left.\frac{\partial \tilde{P}}{\partial C_{i\infty}}\right|_{\Psi_0} \frac{\mathrm{d}C_{i\infty}}{\mathrm{d}X} + \left.\frac{\partial \tilde{P}}{\partial \Psi_0}\right|_{C_{i\infty}} \frac{\partial \Psi_0}{\partial X}, \tag{11}$$

$$\left.\frac{\partial P}{\partial Y}\right|_X = \sum_i \left.\frac{\partial \tilde{P}}{\partial C_{i\infty}}\right|_{\Psi_0} \frac{\partial C_{i\infty}}{\partial Y} + \left.\frac{\partial \tilde{P}}{\partial \Psi_0}\right|_{C_{i\infty}} \frac{\partial \Psi_0}{\partial Y} = \left.\frac{\partial \tilde{P}}{\partial \Psi_0}\right|_{C_{i\infty}} \frac{\partial \Psi_0}{\partial Y}. \tag{12}$$

Comparing Eq. (12) with Eq. (9), we obtain

$$\left.\frac{\partial \tilde{P}}{\partial \Psi_0}\right|_{C_{i\infty}} = \frac{\partial^2 \Psi_0}{\partial Y^2}. \tag{13}$$

Utilizing Eq. (13) in Eq. (11) then results in

$$\left.\frac{\partial P}{\partial X}\right|_Y = \sum_i \left.\frac{\partial \tilde{P}}{\partial C_{i\infty}}\right|_{\Psi_0} \frac{\mathrm{d}C_{i\infty}}{\mathrm{d}X} + \frac{\partial^2 \Psi_0}{\partial Y^2}\frac{\partial \Psi_0}{\partial X}. \tag{14}$$

Now, we focus on the X-direction balance of Eq. (2b). Since both X and Y are $\mathcal{O}(1)$ in the Debye layer, Eq. (2b) can be approximated as

$$\frac{\partial P}{\partial X} = \frac{\partial^2 U_X}{\partial Y^2} + \frac{\partial^2 \Psi_0}{\partial Y^2}\frac{\partial \Psi}{\partial X} \tag{15}$$

Substituting Eq. (14) in Eq. (15) yields

$$\frac{\partial^2 U_X}{\partial Y^2} = -\frac{\partial^2 \Psi_0}{\partial Y^2}\frac{\mathrm{d}\Psi_\infty}{\mathrm{d}X} + \sum_i \left.\frac{\partial \tilde{P}}{\partial C_{i\infty}}\right|_{\hat{\Psi}_0} \frac{\mathrm{d}C_{i\infty}}{\mathrm{d}X}. \tag{16}$$

To the best of our knowledge, the form of Eq. (16) has not been noted previously. Eq. (16) provides insights into the mechanism for motion as it clearly separates the contributions from the bulk electric field (electrophoresis), which is proportional to $\frac{\mathrm{d}\Psi_\infty}{\mathrm{d}X}$, and the electric field energy inside the double layer (chemiphoresis), which is proportional to $\frac{\mathrm{d}C_{i\infty}}{\mathrm{d}X}$.

Next, we integrate Eq. (16) to evaluate the diffusioosmotic slip velocity $U_{\mathrm{DO}} = U_X(X, Y \to \infty)$. Integration of the electrophoretic component is straightforward. We first use Eq. (10) to recognize that $\frac{\partial \tilde{P}}{\partial C_{i\infty}} = g_i(\Psi_0)$, which on substitution into Eq. (16) yields

$$\frac{\partial^2 U_X}{\partial Y^2} = -\frac{\partial^2 \Psi_0}{\partial Y^2}\frac{\mathrm{d}\Psi_\infty}{\mathrm{d}X} + \sum_i g_i(\Psi_0)\frac{\mathrm{d}C_{i\infty}}{\mathrm{d}X}. \tag{17}$$

We integrate this equation once across the double layer subject to the condition that Y-derivatives vanish as $Y \to \infty$ to obtain

$$\frac{\partial U_X}{\partial Y} = -\frac{\partial \Psi_0}{\partial Y}\frac{\mathrm{d}\Psi_\infty}{\mathrm{d}X} + \sum_i \left(\frac{\mathrm{d}C_{i\infty}}{\mathrm{d}X}\int_\infty^Y g_i(\Psi_0(X,Y'))\mathrm{d}Y'\right). \tag{18}$$

Since the chemiphoretic contribution to the velocity distribution depends on Y' only through the excess potential $\Psi_0(X,Y')$, it is convenient to change the integration variable from Y' to Ψ' to find

$$\frac{\partial U_X}{\partial Y} = -\frac{\partial \Psi_0}{\partial Y}\frac{\mathrm{d}\Psi_\infty}{\mathrm{d}X} + \sum_i \left(\frac{\mathrm{d}C_{i\infty}}{\mathrm{d}X}\int_0^{\Psi_0} g_i(\Psi')\left(\frac{\partial \Psi'}{\partial Y'}\right)^{-1}\mathrm{d}\Psi'\right). \tag{19}$$

Similarly, we integrate again across the double layer and utilize the boundary conditions on velocity and potential, i.e. $U_X(X,0)=0$, and $U_X(X,\infty)=U_{\rm DO}$, $\Psi_0(X,0)=\Psi_D$ and $\Psi_0(X,0)=\infty$ to get

$$U_{\rm DO}=\frac{\mathrm{d}\Psi_\infty}{\mathrm{d}X}\Psi_D+\sum_i\left(\frac{\mathrm{d}C_{i\infty}}{\mathrm{d}X}\int_{\Psi_D}^{0}\left[\int_0^{\Psi_0}g_i(\Psi')\left(\frac{\partial\Psi'}{\partial Y}\right)^{-1}\mathrm{d}\Psi'\right]\left(\frac{\partial\Psi_0}{\partial Y}\right)^{-1}\mathrm{d}\Psi_0\right). \tag{20}$$

Finally, we substitute the expression for $\frac{\partial\Psi_0}{\partial Y}$ from Eq. (6) in Eq. (20) to obtain

$$U_{\rm DO}=\frac{\mathrm{d}\Psi_\infty}{\mathrm{d}X}\Psi_D-\frac{1}{2}\sum_i\left(\frac{\mathrm{d}C_{i\infty}}{\mathrm{d}X}\int_0^{\Psi_D}\frac{\left[\int_0^{\Psi_0}g_i(\Psi')\left(\sum_j C_{j\infty}g_j(\Psi')\right)^{-\frac{1}{2}}\mathrm{d}\Psi'\right]}{\left(\sum_j C_{j\infty}g_j(\Psi_0)\right)^{\frac{1}{2}}}\mathrm{d}\Psi_0\right), \tag{21}$$

where we recall that $g_i(\Psi)\equiv\exp(-z_i\Psi)-1$, as given by Eq. (7). Eq. (21) is a statement relating the diffusioosmotic velocity to the excess ion concentration $g_i(\Psi)$ and the energy density of the double layer $\sum_i C_{i\infty}g_i(\Psi)$, albeit a complicated one. To relate $\frac{\mathrm{d}\Psi_\infty}{\mathrm{d}X}$ and $\frac{\mathrm{d}C_{i\infty}}{\mathrm{d}X}$, we now analyse Eqs. (2) in the bulk.

2. Analysis in Bulk

Now, we assume that there is no external electric field applied to the system. We also invoke the condition that the surface conduction effect is negligible, *i.e.* the flux of ions in the direction perpendicular to the surface can be neglected [33]. Hence, in the bulk, the dependence on Y vanishes, or $C_i=C_{i\infty}(X)$, $P=0$ and $\Psi=\Psi_\infty(X)$. In the bulk, $x=\mathcal{O}(a^*)$, or $X=\mathcal{O}(1)$. Thus, for $\delta\to0$, Eq. (2c) yields the electroneutrality conditions

$$\sum_i z_iC_{i\infty}=0. \tag{22}$$

Moreover, since there is no externally applied electric field in diffusiophoresis, the net current in the bulk should be zero, $\sum_i z_iJ_{iX}=0$ [22, 32]. This condition allows us to relate Ψ_∞ to $C_{i\infty}$ by substituting the expression for J_{iX} from Eq. (2e) and summing over the ions to find

$$-\sum_i z_i\mathcal{D}_i\frac{\mathrm{d}C_{i\infty}}{\mathrm{d}X}+\alpha U_{\rm DO}\sum_i z_iC_{i\infty}-\frac{\mathrm{d}\Psi_\infty}{\mathrm{d}X}\sum_i z_i^2\mathcal{D}_iC_{i\infty}=0. \tag{23}$$

Using Eq. (22), Eq. (23) yields [24, 36]

$$\frac{\mathrm{d}\Psi_\infty}{\mathrm{d}X}=-\frac{\sum_i\mathcal{D}_iz_i\frac{\mathrm{d}C_{i\infty}}{\mathrm{d}X}}{\sum_i\mathcal{D}_iz_i^2C_{i\infty}}. \tag{24}$$

We note that Eq. (24) is derived by ignoring surface conduction effects, and in the absence of externally applied electric fields. However, for large Ψ_D, surface conduction effect could be important [32, 33]. In section IV, we summarize typical scenarios encountered in experiments, and discuss when surface conduction effect is likely to be significant. A more comprehensive and rigorous theoretical analysis of this effect for a mixture of multiple ions is feasible within the current framework and should be carried out in future studies.

3. Final Result

We now combine the results from the double layer analysis and the bulk region. Substituting Eq. (24) in (21) yields

$$U_{\rm DO}=-\frac{\sum_i\mathcal{D}_iz_i\frac{\mathrm{d}C_{i\infty}}{\mathrm{d}X}}{\sum_i\mathcal{D}_iz_i^2C_{i\infty}}\Psi_D-\frac{1}{2}\sum_i\left(\frac{\mathrm{d}C_{i\infty}}{\mathrm{d}X}\int_0^{\Psi_D}\frac{\left[\int_0^{\Psi_0}g_i(\Psi')\left(\sum_j C_{j\infty}g_j(\Psi')\right)^{-\frac{1}{2}}\mathrm{d}\Psi'\right]}{\left(\sum_j C_{j\infty}g_j(\Psi_0)\right)^{\frac{1}{2}}}\mathrm{d}\Psi_0\right), \tag{25}$$

where $g_i(\Psi_0)\equiv\exp(-z_i\Psi_0)-1$ and $C_{i\infty}(X)$ needs to satisfy the bulk electroneutrality condition, i.e. $\sum_i z_iC_{i\infty}=0$. We also recall that Ψ_D is dependent on Q through Eq. (8).

Equation (25) is our main result for the diffusioosmotic velocity as a function of the zeta potential Ψ_D of the surface and the bulk ion concentration fields. To the best of our knowledge, the form of this equation has not been reported previously for the case of a general mixture of ions. We emphasize that for the evaluation of U_{DO}, the expression of $\Psi_0(X,Y)$ is not necessary, and integrating terms containing $g_i(\Psi_0)$ is sufficient to evaluate U_{DO}, as evident from Eq. (25).

It is clear from Eq. (25) that for a single salt, both the electrophoretic and chemiphoretic components would be proportional to $\frac{\mathrm{d}\ln C_\infty}{\mathrm{d}X}$. Moreover, since $X=\mathcal{O}(1)$ and $C_{i\infty}=\mathcal{O}(1)$, the electrophoretic and chemiphoretic terms are both $\mathcal{O}(\Psi_D)$. Lastly, the diffusiophoretic velocity U_{DP} is equal and opposite to the value of U_{DO} predicted in Eq. (25), i.e., $U_{\mathrm{DP}}=-U_{\mathrm{DO}}$, in the limit of $\frac{\lambda_D}{b^*}\to 0$, where b^* is the diameter of the particle.

C. The Debye–Hückel Limit of $|\Psi_D| \ll 1$

We now discuss some limiting cases for which the integrals involved in U_{DO} can be evaluated explicitly. For small potentials ($|\Psi_D|\ll 1$), a Taylor series expansion shows that $g_i(\Psi_0)=-z_i\Psi_0+\frac{z_i^2}{2}\Psi_0^2-\frac{z_i^3}{6}\Psi_0^3+\mathcal{O}\left(\Psi_0^4\right)$. Substituting this expression into Eq. (25) and using the electroneutrality condition, we get

$$U_{\mathrm{DO}}=-\frac{\sum_i \mathcal{D}_i z_i \frac{\mathrm{d}C_{i\infty}}{\mathrm{d}X}}{\sum_i \mathcal{D}_i z_i^2 C_{i\infty}}\Psi_D-\frac{\sum_i z_i^2\frac{\mathrm{d}C_{i\infty}}{\mathrm{d}X}}{\sum_i z_i^2 C_{i\infty}}\frac{\Psi_D^2}{8}+\left(\frac{\sum_i z_i^3\frac{\mathrm{d}C_{i\infty}}{\mathrm{d}X}}{\sum_i z_i^2 C_{i\infty}}-\frac{5\left(\sum_i z_i^2\frac{\mathrm{d}C_{i\infty}}{\mathrm{d}X}\right)\left(\sum_i z_i^3 C_{i\infty}\right)}{4\left(\sum_i z_i^2 C_{i\infty}\right)^2}\right)\frac{\Psi_D^3}{54}+\mathcal{O}(\Psi_D^4) \quad (26)$$

Equation (26) provides a convenient expression to evaluate U_{DO} with an order of accuracy $\mathcal{O}(\Psi_D^3)$. If we neglect the cubic term, our result is consistent with previous reports [24, 27], where the authors arrived at their result by utilizing the potential description $\Psi_0(X,Y)$ in the linear limit (the Debye–Hückel approximation) [24]. We also observe that at $O(\Psi_D^3)$, the diffusioosmotic velocity depends explicitly on the difference of magnitude between the anion and cation valences (through z_i^3), which is a qualitatively new effect that is not captured by Debye–Hückel theory.

D. The Limit of $|\Psi_D| \gg 1$

We now develop useful approximations for the case of large potentials $\Psi_D\gg 1$. For $\Psi_D>0$, in any given mixture of ions, we identify the largest anion valence by $z_-=-\max_i(|z_{i-}|)$, and approximate $g_i(\Psi_0)\approx\exp\left(-z_{i-}\Psi_0\right)$. Since, in the chemiphoretic term, z_{i-} appears in the exponential, only anions (i) with $z_{i-}=z_-$ will contribute significantly to summations involved in the chemiphoretic portion of U_{DO}. Thus, we sum only over salts with anion valence z_-, indicated below with a $(-)$ over the sum. The analysis for $\Psi_D<0$ is similar: we identify $z_+=\max_i(z_{i+})$ and sum only over salts with cation valence z_+, indicated below with a $(+)$ over the sum.

Next, we observe from Eq. (25) that evaluating integrals involves the limit from 0 to Ψ_0 or 0 to Ψ_D. The approximation of $g_i(\Psi_0)$ above is inaccurate near the lower integration limit, and can be shown, as a result, to overestimate the integrals by a subdominant $\mathcal{O}(1)$ term for $|\Psi_0|\gg 1$. We correct for this error by modifying the lower limit of the integral in Eq. (25) from 0 to Ψ_ℓ, where Ψ_ℓ is an $\mathcal{O}(1)$ parameter whose value we discuss later. As we will show, the introduction of Ψ_ℓ leaves the leading-order asymptotic behavior of U_{DO} unchanged for $|\Psi_D|\gg 1$, while allowing us obtain a significant improvement in the numerical accuracy of our predictions for moderate zeta potentials $|\Psi_D|\gtrsim 1$.

Thus substituting (i) $g_i(\Psi_0)\approx\exp\left(-z_{i-}\Psi_0\right)$ for $\Psi_D\gg 1$, (ii) $g_i(\Psi_0)\approx\exp\left(-z_{i+}\Psi_0\right)$ for $-\Psi_D\gg 1$, and (iii) modifying the lower limits of integration from 0 to Ψ_ℓ in Eq. (25), we obtain

$$U_{\mathrm{DO}}=\begin{cases}-\dfrac{\sum_i \mathcal{D}_i z_i \frac{\mathrm{d}C_{i\infty}}{\mathrm{d}X}}{\sum_i \mathcal{D}_i z_i^2 C_{i\infty}}\Psi_D+\displaystyle\sum_i^{(+)}\frac{\frac{\mathrm{d}C_{i\infty}}{\mathrm{d}X}}{C_{i\infty}}\left(\frac{\Psi_D+\Psi_\ell}{z_+}-\frac{2\left(\exp\left(z_+(\Psi_\ell+\Psi_D)/2\right)-1\right)}{z_+^2}\right), & -\Psi_D\gg 1\\[2ex] -\dfrac{\sum_i \mathcal{D}_i z_i \frac{\mathrm{d}C_{i\infty}}{\mathrm{d}X}}{\sum_i \mathcal{D}_i z_i^2 C_{i\infty}}\Psi_D-\displaystyle\sum_i^{(-)}\frac{\frac{\mathrm{d}C_{i\infty}}{\mathrm{d}X}}{C_{i\infty}}\left(\frac{\Psi_\ell-\Psi_D}{z_-}+\frac{2\left(\exp\left(-z_-(\Psi_\ell-\Psi_D)/2\right)-1\right)}{z_-^2}\right), & \Psi_D\gg 1.\end{cases} \quad (27)$$

To leading order, observe that the diffusioosmotic velocity is linear in Ψ_D for $|\Psi_D|\gg 1$. The next order is independent of Ψ_D but depends on the $\mathcal{O}(1)$ parameter Ψ_ℓ, for which we determine an approximation in the next section. In section V, we detail the accuracy of the Debye-Hückel limit and the $|\Psi_D|\gg 1$ approximations. We reiterate that our analysis assumes that finite ion size, dielectric decrement and surface conductions effects are negligible, which may become important for $|\Psi_D|\gg 1$, as we detail below.

TABLE I. Summary of physical parameters and relevant dimensionless groups from recent experiments on diffusiophoresis that justify our assumptions. To estimate the values, $d_{\text{ion}} = 3$ Å is assumed for the diameter of an ion (see section IV B) and $\gamma = 10$ $[\text{M}]^{-1}$ is assumed for the dielectric decrement factor for an ion (see section IV C).

Property	Ref. [9]	Ref. [7]	Ref [11]	Ref. [25]
c^*	50 [mM]	50 [mM]	2 [mM]	1 [mM]
a^*	60 [μm]	100 [μm]	500 [μm]	100 [μm]
b^*	200 [nm]	500 [nm]	60 - 1000 [nm]	500 [nm]
λ_D	1.3 [nm]	1.3 [nm]	6.7 [nm]	9.5 [nm]
$\frac{\lambda_D}{a*}$	2.2×10^{-5}	1.3×10^{-5}	1.3×10^{-5}	9.5×10^{-5}
$\frac{\lambda_D}{b*}$	6.7×10^{-3}	2.6×10^{-3}	6.7×10^{-3}- 1.1 $\times10^{-1}$	5.2×10^{-3}
$\frac{1}{z}\ln\left(\frac{1}{d_{\text{ion}}^3 c^*}\right)$	7	7	10	11
$\frac{1}{z}\ln\left(\frac{\varepsilon_w}{\gamma c^*}\right)$	5	5	8	9
$2\ln\left(\frac{b*}{\lambda_D}\right)$	10	12	4 - 10	8

IV. VALIDITY OF DERIVED PREDICTIONS

In this section, we address the validity of the assumptions we invoked during our analysis. Specifically, we discuss the following assumptions: (A) thin double layer, (B) ions are point charges (assumed implicitly through the Nernst-Planck equations, see below for details), (C) electrical permittivity is constant, and (D) surface conduction can be ignored. To facilitate this discussion, we compiled data from some of the previously published experimental studies on diffusiophoresis and estimated the physical parameters along with the relevant dimensionless groups; see Table I.

A. Thin Double Layer

The common thin double layer assumption is central to the validity of our derived relation in Eq. (25). Typically, experiments are conducted on diffusiophoresis (and not diffusioosmosis), *i.e.* the scenario when charged particles move under the presence of a salt gradient while the electrolyte is stationary. In diffusiophoresis, there are three length scales: (i) particle size b^*, (ii) Debye length λ_D, and (iii) the length scale over which the imposed ion concentration decays a^*. To utilize Eq. (25) for describing experiments, in addition to $\frac{\lambda_D}{a^*} = \delta \ll 1$, $\frac{\lambda_D}{b^*} \ll 1$ also needs to be satisfied. Based on previously published experimental studies in Table I, we observe that $\lambda_D = 1 - 10$ nm, $a^* = 100 - 500$ μm and $b^* = 60 - 1000$ nm. The table shows that $\frac{\lambda}{a^*} \lesssim \mathcal{O}\left(10^{-4}\right)$ and $\frac{\lambda}{b^*} \lesssim \mathcal{O}\left(10^{-2}\right)$. Therefore, the thin double layer approximation is applicable to typical experimental scenarios. However, we note than when $b^* \lesssim 100$ nm, $\frac{\lambda}{b^*} \lesssim \mathcal{O}\left(10^{-1}\right)$, and there might be some deviations from the velocities predicted by Eq. (25).

B. Ions are Point Charges

Our analysis utilizes the Nernst–Planck equations, *i.e.* Eqs. (2d)–(2e), to solve for the diffusioosmotic and diffusiophoretic velocities. The Nernst–Planck description assumes that ions are point charges and the volume fraction of ions can be ignored when compared to the volume fraction of solvent [28]. However, for large c^* and Ψ_D, the concentration of surface-attracted ions inside the double layer can be large, and finite ion size effects could become important [26, 28, 29]. The dimensionless number that governs this effect is $d_{\text{ion}}^3 c^*$, where d_{ion} is the diameter of an ion. Physically, this parameter is the dimensionless volume fraction of ions in the bulk. The finite ion size effects are not significant when $|\Psi_D| \lesssim \frac{1}{z}\ln\left(\frac{1}{d_{\text{ion}}^3 c^*}\right)$ [26]. To estimate this value, it is crucial to estimate the value of d_{ion}. Typically, $d_{\text{ion}} \approx 1$ Å, although previous studies have argued that the ion diameter should include the hydration shell, modifying this estimate to $d_{\text{ion}} \approx 3$ Å [28]. Therefore, we assumed that $d_{\text{ion}} = 3$ Å to estimate values. Table I shows that finite ion sizes are not significant for $\Psi_D \lesssim 7$. Since most experiments are performed for particles with $\Psi_D \lesssim 4$, we expect that finite ion size effects are not significant for diffusioosmotic and diffusiophoretic velocity predictions.

C. Electrical Permittivity is Constant

We also assumed that the electrical permittivity ε is constant. However, inside the double layer, the electrical permittivity can decrease due to a large concentration of ions. This effect is known as the dielectric decrement, and, similar to finite ion size, it also becomes significant at large c^* and Ψ_D [26, 30, 31]. Specifically, this effect is not significant when $|\Psi_D| \lesssim \frac{1}{z}\ln\left(\frac{\varepsilon_w}{\gamma c^*}\right)$ [26], where γ is the dielectric decrement factor. To estimate the validity, we assumed $\gamma = 10$ $[\mathrm{M}]^{-1}$ [30]. We show in Table I that for $\Psi_D \lesssim 5$, this effect can be ignored. Therefore, a change in the dielectric constant is unlikely to be significant for typical diffusiophoretic experiments.

D. Surface Conduction

As mentioned previously, within the Poisson-Boltzmann framework, for large Ψ_D, a more careful treatment of the bulk region is required to account for the effect of surface conduction where the currents from the double layer can leak into the bulk region [32, 33]. This effect is not significant for $\Psi_D \lesssim 2\ln\left(\frac{1}{\delta}\right)$ [33]. Table I demonstrates that this effect may not be significant for $\Psi_D \lesssim 10$ and would likely not influence typical experiments in diffusiophoresis and diffusioosmosis.

In addition to the above mentioned assumptions, we note that we have not considered specific ion interactions in our analysis. This effect could be taken into account by assuming a Stern layer near the surface and specifically account for ion interactions [37], and will be pursued in our future work.

V. ONE ELECTROLYTE WITH ASYMMETRIC VALENCES

We now discuss the results from Eq. (25) for the case of a single electrolyte. In this section, we also tabulate diffusiophoretic velocities for some common valence asymmetric electrolytes such $CaCl_2$, Na_2SO_4, $MgCl_2$, and others. Since we focus on the case of a single electrolyte in this section, for further discussion, we omit the i subscript from $C_{i\infty}$, $g_i(\Psi_0)$ etc.

A. Exact Solution

For a solution consisting of a single electrolyte, to maintain electroneutrality, we assume that there is one cation with valence z_+ and one anion with valence z_-. Moreover, to satisfy electroneutrality in the bulk, we write $C_{+\infty} = -z_- C_\infty$ and $C_{-\infty} = z_+ C_\infty$. Utilizing Eqs. (7) and (25), we obtain

$$U_{\mathrm{DO}} = \frac{\mathrm{d}\ln C_\infty}{\mathrm{d}X}\left(-\beta\Psi_D - \frac{1}{2}\int_0^{\Psi_D}\frac{\int_0^{\Psi_0}\left(-z_-\exp\left(-z_+\Psi'\right) + z_+\exp\left(-z_-\Psi'\right) - z_+ + z_-\right)^{1/2}\mathrm{d}\Psi'}{\left(-z_-\exp\left(-z_+\Psi_0\right) + z_+\exp\left(-z_-\Psi_0\right) - z_+ + z_-\right)^{1/2}}\mathrm{d}\Psi_0\right) \tag{28}$$

where $\beta = \frac{\mathcal{D}_+ - \mathcal{D}_-}{z_+\mathcal{D}_+ - z_-\mathcal{D}_-}$. We note that the value of β here is consistent with the idea of a junction potential that is generally suggested for asymmetric diffusivities [38, 39]. We now evaluate Eq. (28) in different limits. For one electrolyte and $z_+ = -z_- = z$, Eq. (28) reduces to the well-known result [6, 27, 35]

$$U_{\mathrm{DO}} = -\frac{\mathrm{d}\ln C_\infty}{\mathrm{d}X}\left[\beta\Psi_D + \frac{4}{z^2}\ln\left(\cosh\left(\frac{z\Psi_D}{4}\right)\right)\right]. \tag{29}$$

B. Analytical Approximations

In the limit of $|\Psi_D| \ll 1$, Eq. (26) or Eq. (28) reduces to

$$\frac{U_{\mathrm{DO}}}{\frac{\mathrm{d}\ln C_\infty}{\mathrm{d}X}} = -\beta\Psi_D - \frac{\Psi_D^2}{8} - \left(z_+ + z_-\right)\frac{\Psi_D^3}{216} + \mathcal{O}(\Psi_D^4). \tag{30}$$

Equation (30) shows that the electrophoresis term is affected by valence through the definition of β. The quadratic terms of the chemiphoretic contribution is independent of the valence whereas the cubic correction is influenced by the difference between the (unsigned) valences of the cation and anion. For $|\Psi_D| \gg 1$, Eq. (27) reduces to

$$\frac{U_{\mathrm{DO}}}{\frac{\mathrm{d}\ln C_\infty}{\mathrm{d}X}} = \begin{cases} -\beta\Psi_D + \left(\dfrac{\Psi_D+\Psi_\ell}{z_+} - \dfrac{2\left(\exp\left(z_+(\Psi_\ell+\Psi_D)/2\right)-1\right)}{z_+^2}\right), & -\Psi_D \gg 1 \\ -\beta\Psi_D - \left(\dfrac{\Psi_\ell-\Psi_D}{z_-} + \dfrac{2\left(\exp\left(-z_-(\Psi_\ell-\Psi_D)/2\right)-1\right)}{z_-^2}\right), & \Psi_D \gg 1. \end{cases} \tag{31}$$

Therefore, as $|\Psi_D|$ increases, the impact of asymmetry in cation and anion valences on the chemiphoretic contribution also increases. Comparing the approximation (31) with the exact solution (29) for large zeta potentials, we find that the two expressions agree identically at leading (linear) order in Ψ_D. Subdominant terms in both expressions are $\mathcal{O}(1)$; requiring agreement at this order determines the parameter

$$\Psi_\ell = \begin{cases} z_+^{-1}\left(4\ln 2 - 2\right), & -\Psi_D \gg 1 \\ -z_-^{-1}\left(4\ln 2 - 2\right), & \Psi_D \gg 1. \end{cases} \tag{32}$$

With these choices for Ψ_ℓ, (31) and (29) differ only by a terms exponentially small in $|\Psi_D|$. We note that the Ψ_ℓ values determined above are formally valid for a single $z:z$ electrolyte, though we expect them to provide reasonable approximations for more complicated situations such as mixtures of valence-asymmetric electrolytes (Fig. 2 and appendix A). We reiterate that the leading-order behaviour of our approximation Eq. (31) for large potentials remains independent of Ψ_ℓ.

C. Validity of Analytical Approximations

We now present the variation of U_{DO} by numerically integrating the exact expression Eq. (28) for some typical $z_+:z_-$ electrolytes, and discuss the accuracy and applicability of approximations Eqs. (30)–(31). The properties of common electrolytes are summarized in Table II, and typical results for U_{DO} are shown in Fig. 2. We find that though Eq. (30) is derived for $|\Psi_D| \ll 1$, it is a good approximation of the exact result from Eq. (28) for $|\Psi_D| \lesssim 1$; see Fig. 2(a). However, we discover that Eq. (30) with accuracy up to $\mathcal{O}(\Psi_D^3)$ is closer to the numerical results as compared to Eq. (30) with accuracy only up to $\mathcal{O}(\Psi_D^2)$ for all Ψ_D, depending on the value of β, z_+, and z_-. Therefore, the improvements due to higher-order corrections are restricted for larger $|\Psi_D|$ and Eq. (30) should be utilized for $|\Psi_D| \lesssim 1$. In contrast, Eq. (31) gives a more accurate predication for larger $|\Psi_D|$ and is best utilized for $|\Psi_D| \gtrsim 4$, though in many cases can also provide good approximations for smaller potentials; see Fig. 2(b). We note that before utilizing Eq. (31), it should be ensured that effects such as finite ion size, dielectric decrement and surface conduction are not significant. The results in Fig. 2(b) were generated using the values of Ψ_ℓ provided in Eq. (32). We discuss the sensitivity of our results on the choice of Ψ_ℓ in the appendix A. We emphasize that z_+ and z_- significantly influence U_{DO}, as evident from Eq. (31) and Fig. 2(a,b).

D. Some Common $z_+:z_-$ Electrolytes

We now present a comparison of U_{DO} for different electrolytes and the results are summarized in Fig. 3. We first compare HCl and H_2SO_4. Since the cation is H^+ in these two electrolytes, β values are large and positive in both cases. For small $|\Psi_D|$, the ratio of electrophoretic and chemiphoretic contributions is $\frac{8\beta}{\Psi_D}$, see Eq. (30). Therefore, for

TABLE II. Values of z_+, z_-, D_+, D_- and β for some common electrolytes at 25°C. The ion diffusivities are taken from [27].

electrolyte	z_+	z_-	D_+ $[10^{-9}\ \mathrm{m^2 s^{-1}}]$	D_- $[10^{-9}\ \mathrm{m^2 s^{-1}}]$	β
HCl	1	-1	9.31	2.03	0.64
H_2SO_4	1	-2	9.31	1.06	0.72
NaCl	1	-1	1.33	2.03	−0.21
Na_2SO_4	1	-2	1.33	1.06	0.08
$CaCl_2$	2	-1	0.79	2.03	−0.34
$Mg(HCO3)_2$	2	-1	0.70	1.18	−0.18

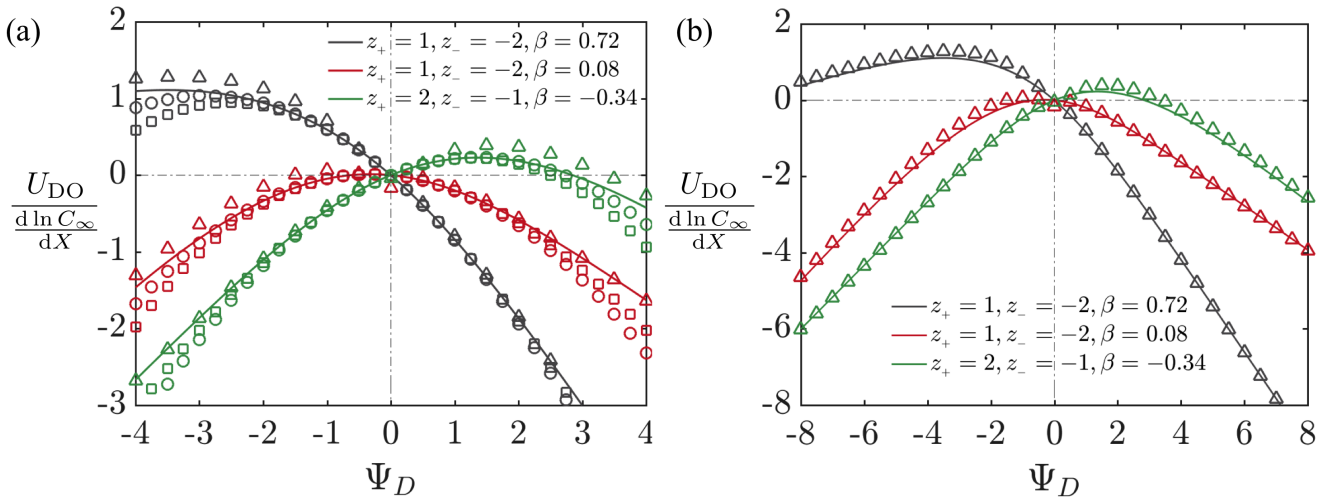

FIG. 2. Approximate solutions for the diffusioosmotic velocity as compared to predictions Eq. (28), calculated by numerical integration. The solid lines are the results of numerically integrating Eq. (28), circles are results from Eq. (30) with accuracy upto $\mathcal{O}(\Psi_D^2)$, squares are evaluated through Eq. (30) with accuracy upto $\mathcal{O}(\Psi_D^3)$, and triangles are generated from Eq. (31) with Ψ_ℓ values given by Eq. (32). The parameters $z_+ = 1, z_- = -2, \beta = 0.72$ correspond to H_2SO_4, $z_+ = 1, z_- = -2, \beta = 0.08$ correspond to Na_2SO_4, and $z_+ = 2, z_- = -1, \beta = -0.34$ correspond to $CaCl_2$; see Table II.

HCl and H_2SO_4, the two contributions are cooperative for $\Psi_D > 0$ and competitive for $\Psi_D < 0$. Next, we compare NaCl and Na_2SO_4. Though the cation for both of these electrolytes is same, due to the smaller diffusivity of SO_4^{2-} as compared to Cl^-, and because the valence of SO_4^{2-} is higher, there is a considerable difference between the β values of the two electrolytes (see Table II). We find that since β is negative for NaCl, for $\Psi_D > 0$, the electrophoretic and chemiphoretic components compete with each other. In contrast, since the electrophoretic effect is weak for Na_2SO_4, for $\Psi_D > 0$, the diffusioosmotic velocity of Na_2SO_4 is larger in magnitude as compared to NaCl. However, the opposite is true for $\Psi_D < 0$, where for NaCl, the electrophoretic and chemiphoretic components are similarly signed and thus the case of NaCl has a larger magnitude of diffusioosmotic velocity as compared to Na_2SO_4. A similar comparison can be drawn between $CaCl_2$ and $Mg(HCO_3)_2$. These examples demonstrate that asymmetric valence electrolytes can be utilized for control over diffusioosmotic and diffusiphoretic processes, and may influence other electrokinetic phenomena.

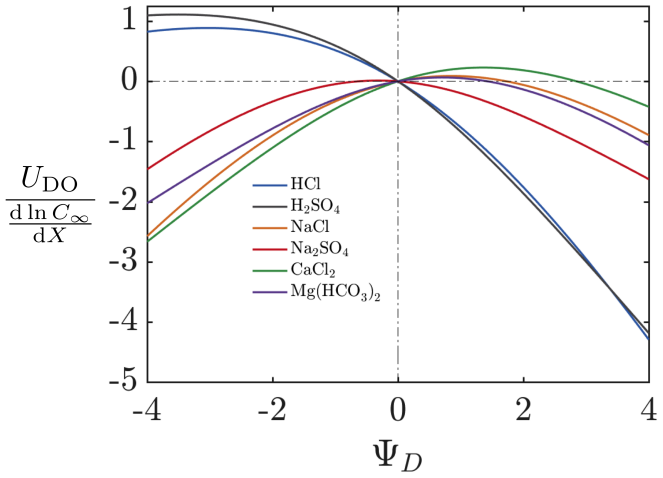

FIG. 3. Diffusioosmotic velocity for some common $z:z$ and $z_+:z_-$ electrolytes as given by Eq. (28).

VI. CONCLUSIONS

In this article, we presented general results for diffusioosmotic and diffusiophoretic velocities for a mixture of valence-asymmetric electrolytes with arbitrary z_i. Equation (25) includes the effect of valence asymmetry for a mixture of electrolytes, and Eq. (28) describe the dependence for a single electrolyte. We also presented the approximate solutions in the limit of $|\Psi_D| \ll 1$ and $|\Psi_D| \gg 1$; see Eqs. (26), (27), (30) and (31). We demonstrated that asymmetry in electrolyte valence is a useful parameter to tune the diffusiophoretic and diffusioosmotic motions. Our analysis will motivate future experimental studies on diffusiophoresis and diffusioosmosis using mixture of electrolytes and multivalent salts. Future theoretical studies in this area could focus on including the effects of finite ion size, dielectric decrement and surface conduction in the analysis to further generalize diffusiophoretic and diffusioosmostic velocity relations.

ACKNOWLEDGEMENTS

We thank the financial support from the Andlinger Center for Energy and the Environment at Princeton University and the NSF via grant CBET - 1702693. We thank Suin Shin and Jessica L. Wilson for useful discussions. We also acknowledge the two anonymous referees for their comments and suggestions as they were crucial to significantly improving our manuscript.

Appendix A: The Choice of Ψ_ℓ

We now discuss the dependence of $U_{\rm DO}$ on Ψ_ℓ when Eq. (31) is utilized to evaluate $U_{\rm DO}$. We find that Ψ_ℓ from Eq. (32) provides the best approximation to the numerical solution as compared to other values; see Fig. A1. However, all values of Ψ_ℓ between 0 and 1 work reasonably well. However, for larger values of Ψ_ℓ, such as $\Psi_\ell = 5$, the deviation from the numerical solution is significant.

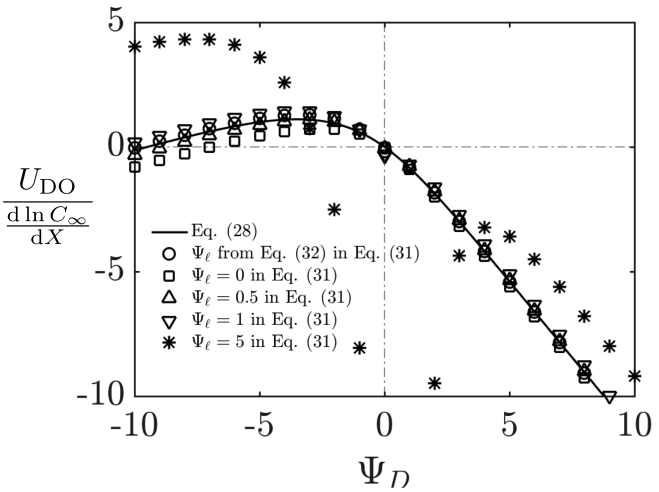

FIG. A1. Comparison of $U_{\rm D0}$ obtained from Eq. (31) with numerical solution of Eq. (28) for different values of Ψ_ℓ. Parameter values of $\beta = 0.72$, $z_+ = 1$ and $z_- = -2$ (corresponding to H_2SO_4) were used.

[1] Bazant, M. Z., Thornton, K., and Ajdari, A. Diffuse-charge dynamics in electrochemical systems. *Phys. Rev. E*, 70(2): 021506, 2004.
[2] Simon, P. and Gogotsi, Y. Materials for electrochemical capacitors. *Nat. Mater.*, 7:845–854, 2008.
[3] Dukhin, S. S. Non-equilibrium electric surface phenomena. *Adv. Colloid Interface Sci.*, 44:1–134, 1993.

[4] Anderson, J. L. and Idol, W. K. Electroosmosis through pores with nonuniformly charged walls. *Chem. Eng. Commun.*, 38(3-6):93–106, 1985.

[5] Anderson, J. L. Colloid transport by interfacial forces. *Annu. Rev. Fluid Mech.*, 21(1):61–99, 1989.

[6] Prieve, D., Anderson, J., Ebel, J., and Lowell, M. Motion of a particle generated by chemical gradients. Part 2. Electrolytes. *J. Fluid Mech.*, 148:247–269, 1984.

[7] Kar, A., Guha, R., Dani, N., Velegol, D., and Kumar, M. Particle deposition on microporous membranes can be enhanced or reduced by salt gradients. *Langmuir*, 30(3):793–799, 2014.

[8] Raşa, M. and Philipse, A. P. Evidence for a macroscopic electric field in the sedimentation profiles of charged colloids. *Nature*, 429(6994):857, 2004.

[9] Abécassis, B., Cottin-Bizonne, C., Ybert, C., Ajdari, A., and Bocquet, L. Boosting migration of large particles by solute contrasts. *Nat. Mat.*, 7(10):785, 2008.

[10] Shin, S., Shardt, O., Warren, P. B., and Stone, H. A. Membraneless water filtration using CO_2. *Nat. Comm.*, 8:15181, 2017.

[11] Shin, S., Um, E., Sabass, B., Ault, J. T., Rahimi, M., Warren, P. B., and Stone, H. A. Size-dependent control of colloid transport via solute gradients in dead-end channels. *Proc. Nat. Acad. Sc.*, 113(2):257–261, 2016.

[12] Kar, A., Chiang, T.-Y., Ortiz Rivera, I., Sen, A., and Velegol, D. Enhanced transport into and out of dead-end pores. *ACS Nano*, 9(1):746–753, 2015.

[13] Palacci, J., Abécassis, B., Cottin-Bizonne, C., Ybert, C., and Bocquet, L. Colloidal motility and pattern formation under rectified diffusiophoresis. *Phys. Rev. Lett.*, 104(13):138302, 2010.

[14] Palacci, J., Cottin-Bizonne, C., Ybert, C., and Bocquet, L. Osmotic traps for colloids and macromolecules based on logarithmic sensing in salt taxis. *Soft Matter*, 8(4):980–994, 2012.

[15] Frankel, A. E. and Khair, A. S. Dynamics of a self-diffusiophoretic particle in shear flow. *Phys, Rev. E*, 90(1):013030, 2014.

[16] Nery-Azevedo, R., Banerjee, A., and Squires, T. M. Diffusiophoresis in ionic surfactant gradients. *Langmuir*, 33(38): 9694–9702, 2017.

[17] Shin, S., Warren, P. B., and Stone, H. A. Cleaning by surfactant gradients: Particulate removal from porous materials and the significance of rinsing in laundry detergency. *Phys. Rev. Appl.*, 9(3):034012, 2018.

[18] Reinmüller, A., Schöpe, H. J., and Palberg, T. Self-organized cooperative swimming at low Reynolds numbers. *Langmuir*, 29(6):1738–1742, 2013.

[19] Brown, A. T. and Poon, W. C. Ionic effects in self-propelled Pt-coated janus swimmers. *Soft Matter*, 10(22):4016–4027, 2014.

[20] Brown, A. T., Poon, W. C., Holm, C., and de Graaf, J. Ionic screening and dissociation are crucial for understanding chemical self-propulsion in polar solvents. *Soft Matter*, 13(6):1200–1222, 2017.

[21] Shin, S., Ault, J. T., Feng, J., Warren, P. B., and Stone, H. A. Low-cost zeta potentiometry using solute gradients. *Adv. Mat.*, 29(30):1701516, 2017.

[22] Prieve, D. C. and Roman, R. Diffusiophoresis of a rigid sphere through a viscous electrolyte solution. *Journal of the Chemical Society, Faraday Transactions 2: Molecular and Chemical Physics*, 83(8):1287–1306, 1987.

[23] Gouy, M. Sur la constitution de la charge électrique à la surface d'un électrolyte. *J. Phys. Theor. Appl.*, 9(1):457–468, 1910.

[24] Chiang, T.-Y. and Velegol, D. Multi-ion diffusiophoresis. *J. Colloid Interface Sci.*, 424:120–123, 2014.

[25] Shi, N., Nery-Azevedo, R., Abdel-Fattah, A. I., and Squires, T. M. Diffusiophoretic focusing of suspended colloids. *Phys. Rev. Lett.*, 117(25):258001, 2016.

[26] Gupta, A. and Stone, H. A. Electrical double layers: Effect of asymmetry in electrolyte valence on steric effects, dielectric decrement and ion-ion correlations. *Langmuir*, 34:11971–11985, 2018.

[27] Velegol, D., Garg, A., Guha, R., Kar, A., and Kumar, M. Origins of concentration gradients for diffusiophoresis. *Soft Matter*, 12(21):4686–4703, 2016.

[28] Kilic, M. S., Bazant, M. Z., and Ajdari, A. Steric effects in the dynamics of electrolytes at large applied voltages. I. Double-layer charging. *Phys. Rev. E*, 75(2):021502, 2007.

[29] Kilic, M. S., Bazant, M. Z., and Ajdari, A. Steric effects in the dynamics of electrolytes at large applied voltages. II. Modified Poisson-Nernst-Planck equations. *Phys. Rev. E*, 75(2):021503, 2007.

[30] Nakayama, Y. and Andelman, D. Differential capacitance of the electric double layer: The interplay between ion finite size and dielectric decrement. *J. Chem. Phys.*, 142(4):044706, 2015.

[31] Hatlo, M. M., Van Roij, R., and Lue, L. The electric double layer at high surface potentials: The influence of excess ion polarizability. *EPL*, 97(2):28010, 2012.

[32] Pawar, Y., Solomentsev, Y. E., and Anderson, J. L. Polarization effects on diffusiophoresis in electrolyte gradients. *Journal of Colloid and Interface Science*, 155(2):488–498, 1993.

[33] Schnitzer, O. and Yariv, E. Macroscale description of electrokinetic flows at large zeta potentials: nonlinear surface conduction. *Physical Review E*, 86(2):021503, 2012.

[34] O'Brien, R. W. and White, L. R. Electrophoretic mobility of a spherical colloidal particle. *Journal of the Chemical Society, Faraday Transactions 2: Molecular and Chemical Physics*, 74:1607–1626, 1978.

[35] Keh, H. J. and Ma, H. C. Diffusioosmosis of electrolyte solutions along a charged plane wall. *Langmuir*, 21(12):5461–5467, 2005.

[36] Deen, W. M. *Analysis of Transport Phenomena*. Oxford University Press, New York, 2012.

[37] Lyklema, J. *Fundamentals of Interface and Colloid Science*, volume 2. Academic Press, 1995.

[38] Persat, A. and Santiago, J. G. An ohmic model for electrokinetic flows of binary asymmetric electrolytes. *Curr. Opin. Colloid Interface Sci*, 24:52–63, 2016.
[39] Hickman, H. J. The liquid junction potential—the free diffusion junction. *Chem. Eng. Sci.*, 25(3):381–398, 1970.